Chinese Chemical Letters 36 (2025) 110593

Contents lists available at ScienceDirect

Chinese Chemical Letters

journal homepage: www.elsevier.com/locate/cclet

Indium-captured zirconium-porphyrin frameworks displaying rare multi-selectivity for catalytic transfer hydrogenation of aldehydes and ketones

Hua Liu[a,1], Jian Zhao[b,1], Qi Li[b], Xiang-Yu Zhang[a,b,*], Zhi-Wei Zheng[a], Kun Huang[a], Da-Bin Qin[a,*], Bin Zhao[a,b,*]

[a] Key Laboratory of Chemical Synthesis and Pollution Control of Sichuan Province, College of Chemistry and Chemical Engineering, China West Normal University, Nanchong 637002, China
[b] Frontiers Science Center for New Organic Matter, Key Laboratory of Advanced Energy Materials Chemistry (MOE), College of Chemistry, Nankai University, Tianjin 300071, China

ARTICLE INFO

Article history:
Received 29 July 2024
Revised 23 October 2024
Accepted 29 October 2024
Available online 30 October 2024

Keywords:
Metal-organic framework
Heterogeneous catalysis
Transfer hydrogenation
Multiple selectivity
Synergistic effect

ABSTRACT

Selective catalytic transfer hydrogenation (CTH) of carbonyl compounds to obtain specific alcohols holds significant importance across various fields. Achieving multiple selectivity in CTH is particularly crucial, but full of great challenge. Herein, a cationic In-captured Zr-porphyrin framework (**1**) with nanosized pores/cages was successfully constructed and showed high structure stability. Catalytic investigations revealed that **1** displayed highly multi-selective CTH of aldehydes and ketones containing both chemo- and size selectivity for the first time. The CTH of aldehydes and ketones exhibited remarkable reductive selectivity of 99% towards C=O bonds into CH–OH in the presence of -NO_2, -CN and C=C groups. Through tuning the reaction conditions, **1** also exhibited highly selective reduction of 97% for -CHO groups in the simultaneous presence of -CHO and -$COCH_3$ groups in intra- and intermolecular settings. Remarkably, reductive selectivity towards -CHO group remained prominent among five concurrent unsaturated groups mentioned above. Additionally, the definite pore size of **1** facilitated volume control of substrates, enabling size selectivity. **1** as a heterogeneous catalyst was further confirmed by leaching tests, and maintained high activity even after being used for at least six cycles. Mechanistic studies have revealed that Zr_6O_8 clusters served as the catalytic centers and the observed chemoselectivity mainly results from the synergistic effect of distinct metal sites within **1**. The heightened selectivity towards -CHO over -$COCH_3$ can be attributed to the easier realization of transfer hydrogenation processes for -CHO compared to -$COCH_3$.

Selective hydrogenation displays significant importance in various domains, including organic synthesis, drug manufacturing, and industrial production [1–3]. This valuable topic focuses on preserving specific functional groups or selecting distinct substrates, meeting the specific requirements in these fields mentioned above [4–7]. Compared with traditional direct hydrogenation, catalytic transfer hydrogenation (CTH) using renewable and sustainable liquids such as alcohols and formates as hydrogen sources, avoids the need for flammable H_2 gas with high pressure and promotes the selectivity of unsaturated bonds [8]. Recent achievements have witnessed impressive progress in CTH reactions [9,10], and selective CTH of furfural, alkenes and α,β-unsaturated carbonyls have been widely studied [11–13]. Since most chemicals in nature or generated from biomass commonly maintain multi-unsaturated groups like -CHO, -COR, -NO_2, -CN and C=C bonds, highly selective reduction aimed at a specific group ensures the generation of definite products preserving other unsaturated groups, which is crucial for realizing advanced functions in the areas of pharmaceutical and chemical industry. Nevertheless, the investigations on selective CTH mainly focused on reduction of the given group in two types of unsaturated groups, while the selective reduction of a specific functional group amongst many kinds of unsaturated groups remains undeveloped [14,15]. Actually, the π-bonds within unsaturated groups are generally easy to be unselectively reduced, and selective CTH frequently confronts the confusion, where the

* Corresponding authors.
E-mail addresses: xyzhang@cwnu.edu.cn (X.-Y. Zhang), qdbkyl@cwnu.edu.cn (D.-B. Qin), zhaobin@nankai.edu.cn (B. Zhao).
[1] These authors contributed equally to this work.

https://doi.org/10.1016/j.cclet.2024.110593
1001-8417/

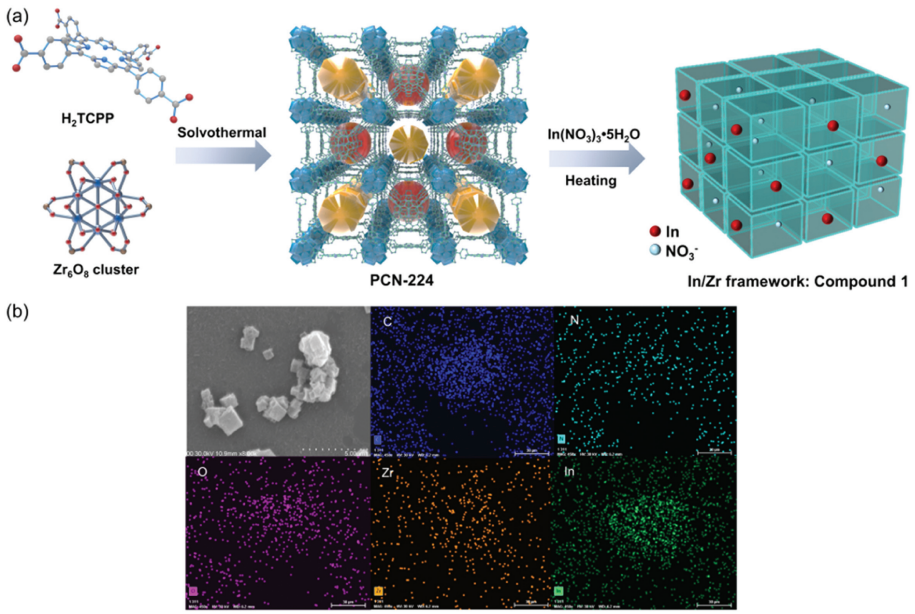

Fig. 1. (a) Synthetic schematic of **1**, (b) SEM and EDS images of **1**.

high activity of catalysts promotes thorough reduction of all unsaturated bonds and inert activity results in an ineffective reaction. As a result, the selective reduction of a single group among various unsaturated groups become greatly challenging [16]. Furthermore, size selectivity enables the screening of substrates with specific volumes for reactions [17–19], and to our best knowledge no size selectivity has been reported in CTH reactions hitherto. Therefore, to realize selective CTH with both definite chemoselectivity among many kinds of unsaturated groups and size selectivity for various substrates, the exploration of an ideal catalyst with suitable catalytic activity and defined pore size is necessary and important.

Metal-organic frameworks (MOFs) constitute a significant category of porous materials that find widespread use as heterogenous catalysts [20–29], and are regarded as candidates for achieving efficient and multi-selective CTH reactions based on the following considerations: (1) Porous structures provide reaction space and allow full utilization of catalytic sites, thus accelerating reaction rate [30–35]; (2) Multi-metallic sites can activate different functional groups, leading to selectivity of specific reaction sites [36–39]; (3) Fixed orifice size enables spatial confinement and presents potentially size-selective properties [40,41]; (4) Stable frameworks make the catalysts easily separated from the reaction mixture and reused several times [42–44]. Despite the numerous advantages of using MOFs as catalysts for CTH reactions, there has been little research on their ability to achieve multiple selectivity, including chemoselectivity towards diverse functional groups and size selectivity [11,45].

With this in mind, a nanopore-based In-captured Zr-porphyrin framework (**1**) was successfully synthesized. In the structure, Zr_6O_8 clusters induce electrons from central metals over the porphyrin skeletons, enhancing the Lewis acidity of the In centers to facilitate the substrate into the pores and interact [46,47]. In CTH reactions of aldehydes and ketones, the dual metal centers in **1** can serve as divided active sites to give definite reductive selectivity towards -CHO or -$COCH_3$ when existing -NO_2, -CN, C=C groups, and note that high selectivity can be also obtained for reduction of -CHO to -CH_2OH in the simultaneous presence of -CHO and -$COCH_3$ groups. Interestingly, when five unsaturated groups mentioned above were concurrently introduced to the CTH system, **1** exhibited a high reductive selectivity towards the -CHO group. Additionally, the specific pore size of **1** afforded volume control of the substrates to give obvious size selectivity. It is the first time to realize highly multi-selective CTH reactions of aldehydes and ketones containing selectivity from various unsaturated groups and volume size confinement.

1 was first synthesized *via* the reaction between Zr-porphyrin framework PCN-224 and $In(NO_3)_3{\cdot}5H_2O$ in DMF (Fig. 1a). Scanning electron microscopy (SEM) images show the block morphology of **1**, and EDS mapping analysis indicates homogeneous distribution of C, N, O, Zr and In elements on the surface (Fig. 1b and Fig. S1 in Supporting information). The elemental amount determined by ICP-OES analysis suggested a 5.78% weight of In in the structure (calcd. 7.77%). In the compared PXRD patterns, the peaks match well with those of PCN-224 and PCN-224(Bi) at 4.6°, 6.4°, 7.9° and 9.0°, as reported previously [47], indicating the scaffold unchanged (Fig. S2 in Supporting information). FT-IR spectrum of **1** is also compared with those of PCN-224 and PCN-224(Bi), and the peak located at 1709.8 cm^{-1} related to carboxylic C=O bond is nearly the same, suggesting the Zr_6O_8 cluster remained unchanged (Fig. S3 in Supporting information). The N–H peak at 3324.2 cm^{-1} disappears, indicating the In-N bond formation. X-ray photoelectron spectroscopy (XPS) results are shown in Fig. 2 and Fig. S4 (Supporting information), and the survey spectrum suggests the existence of In, Zr, N, C and O elements (Fig. 2a). Two typical peaks located at 452.9 and 445.4 eV in In 3d region are related to In $3d_{3/2}$ and $3d_{5/2}$ electronic configurations, respectively, indicating the In^{3+} state (Fig. 2b) [48]. The signals at 185.3 eV ($3d_{3/2}$) and 182.9 eV ($3d_{5/2}$) in Zr 3d spectrum confirm the existence of Zr^{4+} ions (Fig. 2c) [48]. In N 1s spectrum, the peaks at 399.9 and 397.8 eV are attributed to C=N/C–N bonds of porphyrin moiety and In-N bonds, and 407.3 eV signal can be assigned to NO_3^-, indicating that **1** is a cationic framework (Fig. 2d) [49]. With respect to C 1s, three signals at 288.8, 285.9 and 284.8 eV can be attributed to C–O/C=O, C–N/C=N and C–C/C=C bonds (Fig. S4a in Supporting information) [50]. The O 1s peaks located at 533.1, 531.9 and 530.3 eV are correlated to C–O, C=O and Zr-O bonds (Fig. S4b in Supporting information) [51]. TGA curve is depicted in Fig. S5 (Supporting information), and the swift weight reduction of 10% observed prior to reaching 85 °C can be ascribed to solvent evaporation. A reposeful platform with only 15% weight loss is obtained from 85 °C to even 409 °C, showing excellent thermal stability of **1**. After 409 °C, a sharp weight decline suggests the

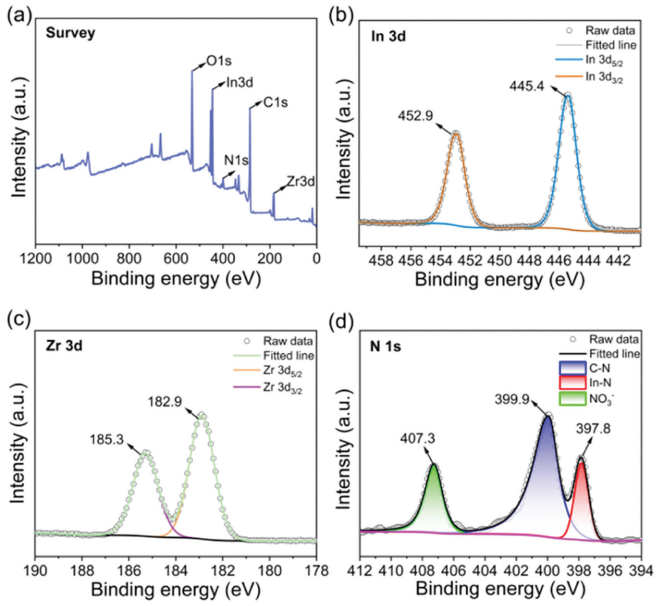

Fig. 2. XPS analysis of **1**: (a) Survey spectrum, (b-d) In 3d, Zr 3d and N 1s spectra.

decomposition of **1**. The analytic results above verify the successful construction of In-captured Zr-porphyrin framework **1**, and porphyrins with In occupied in centers were linked by Zr_6O_8 clusters in this compound [47]. Additionally, the substrate framework PCN-224 featuring nanosized pores/cages of approximately 16 Å, along with 2.2 nm average pore size of **1** (Fig. S6 in Supporting information), provides ample space for diverse organic molecules to approach the catalytic centers, and also possible to realize the size confinement towards these substrates.

Comparatively, the reduction of -NO_2 to -NH_2 in nitrobenzene (redox potential: −1.31 eV) is considered easier than the reduction of -CHO to -CH_2OH in benzaldehyde (redox potential: −1.68 eV) theoretically [12]. As demonstrated in previous research studies, for nitrobenzaldehydes, -NO_2 and -CHO are together reduced to give aminobenzyl alcohols, or -NO_2 are selectively transferred into -NH_2 to afford aminobenzaldehydes in most direct hydrogenation and transfer hydrogenation systems [52–54]. However, in our research, using **1** as a catalyst and isopropanol (*i*PrOH) as the hydrogen source, 4-nitrobenzaldehyde (**1a**) can be selectively reduced to 4-nitrobenzyl alcohol (**2a**) while preserving the -NO_2 group entirely (Table 1, entry 1). In contrast, -NO_2 was also hydrogenated to -NH_2 meanwhile in most MOF-based catalytic system when a strong base was used as an additive [45]. 5,10,15,20-Tetrakis(4-carboxyphenyl)porphyrin-In (In-TCPP) afforded no reductive product under the same conditions and PCN-224 showed lower yield than catalyst **1**, suggesting obvious synergistic effect of two moieties within the catalyst in this reaction (entries 2–3). When a mixture of $In(NO_3)_3{\cdot}5H_2O$, H_2TCPP and $ZrCl_4$ was used, only 35% yield of **2a** was presented, indicating efficient activity of the MOF catalyst (entry 4). The performance of other metals associated with the porphyrin center, such as PCN-224(M) (M= Co, Ni, Bi) was also compared. These selected MOFs showed lower efficiency than compound **1**, suggesting the essential role of the In center within the porphyrin ring. Based on the results above and the optimations in Tables S1-S4 (Supporting information), **1** exhibited high activity and selectivity in CTH of **1a** and was further used as the catalyst for subsequent investigations.

Table 1
Catalyst optimization for selective CTH of 4-nitrobenzaldehyde.[a]

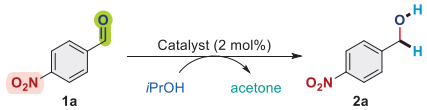

Entry	Catalyst	Yield (%)
1	Catalyst **1**	95
2	In-TCPP	<5
3	PCN-224	83
4	$In(NO_3)_3{\cdot}5H_2O$ +H_2TCPP+$ZrCl_4$	35
5	PCN-224(Co)	77
6	PCN-224(Ni)	35
7	PCN-224(Bi)	81

[a] Reaction conditions: catalyst (2 mol%), *i*PrOH (2 mL), 80 °C, 2 h, the yields were determined as an average value of three runs by ^{1}H NMR analysis.

Compared with aldehydes, ketones need an elevated temperature of 120 °C to afford the desired secondary alcohol products in ideal results (Tables S5-S9 in Supporting information), and higher activity of catalyst **1** over PCN-224 also indicated the significant role of In-TCPP moiety. C=O bond was also reduced selectively for 4-nitroacetophenone (**3a**) with -NO_2 remained and the yield of **4a** is 97% (Fig. 3a). -CN group can be hydrogenated to -CH=NH, -$CONH_2$ or -CH_2NH_2 under H_2 hydrogenation or *via* CTH. Theoretically, -CN group is more easily reduced than C=O bonds due to the lower reduction potential (-CHO, −1.68; -$COCH_3$, −1.75; -CN, −1.29) [55,56]. In the **1** catalytic transfer hydrogenation of 4-cyanobenzaldehyde (**1b**) and 4-cyanoacetophenone (**3b**), C=O bonds were selectively reduced while -CN remained completely, and the alcohols **2b** and **4b** were obtained in high yields (Fig. 3b). As is well-known, the selective reduction of α,β-unsaturated aldehydes and ketones is a significant research focus, cause allylic alcohols are highly vital compounds in many fields [13]. However, in these substrates, C=C bonds also exhibit high reactivity towards reduction, thus it is still a challenge to control the selectivity for C=C and C=O bonds. Attractively, based on catalyst **1**, cinnamalde-

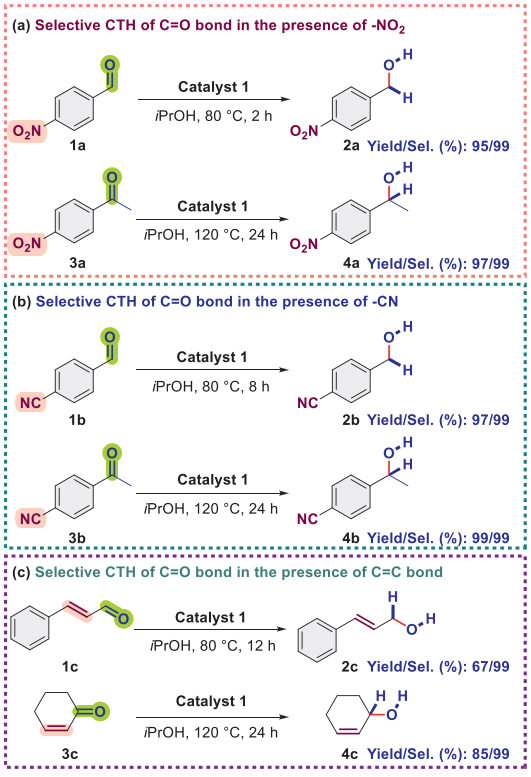

Fig. 3. Selective CTH of C=O bonds in the presence of (a) -NO_2, (b) -CN and (c) C=C bonds.

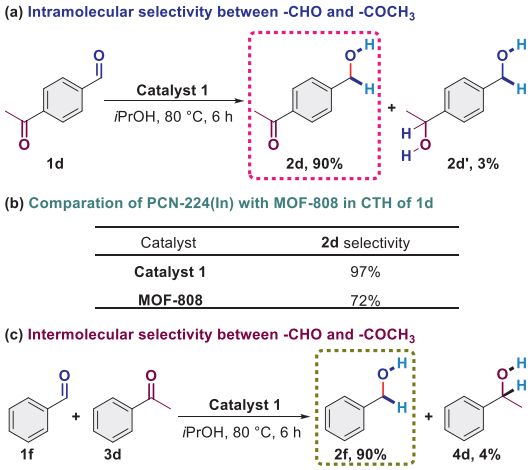

Fig. 4. (a-c) Intra- and intermolecular CTH selectivity between -CHO and -$COCH_3$.

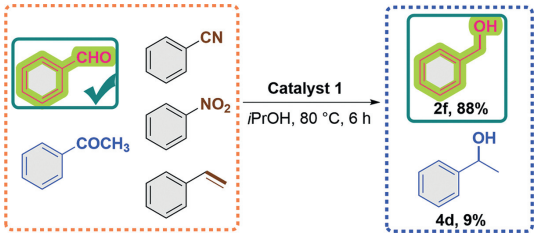

Fig. 5. Selective CTH of -CHO among various unsaturated groups.

hyde (**1c**) produced cinnamyl alcohol (**2c**) and cyclohexanone (**3c**) afforded cyclohexanol (**4c**), maintaining complete selectivity for the reduction of C=O bonds while leaving the C=C bonds unaffected (Fig. 3c). The results above indicate superior reductive selectivity towards the C=O bonds of aldehydes and ketones into CH–OH in the presence of -NO_2, -CN and C=C groups.

In addition to the high selectivity between C=O bonds and the three groups mentioned above, we also conducted investigations into CTH reactions involving the simultaneous presence of -CHO and -$COCH_3$ groups. As we know, -CHO and -$COCH_3$ are similar groups, selective distinction between these two groups is challenging and has an important role in practical applications [57]. To our delight, as shown in Fig. 4a, **1** catalyzed transfer hydrogenation of 4-acetylbenzaldehyde (**1d**) smoothly in 93% yield using *i*PrOH solvent at 80 °C for 6 h. The -CHO reductive product 4-acetylbenzyl alcohol (**2d**) occupied 90%, and the complete reduction product **2d'** was only 3%, showing high reductive selectivity of 97% towards -CHO. In contrast, another Zr_6O_8 cluster-based MOF-808 exhibited a selectivity of only 72% for **2d** under the same condition (Fig. 4b). When benzaldehyde (**1f**) and acetophenone (**3d**) were both introduced to the reaction, benzyl alcohol (**2f**) and 1-phenylethanol (**4d**) were afforded in 90% and 4% yields, respectively (Fig. 4c). The results revealed a notable preference for the selective reduction of the -CHO group over -$COCH_3$, regardless of whether it was present in an intermolecular or intramolecular context.

Remarkably, upon introducing a blend of benzonitrile, acetophenone, nitrobenzene, styrene, and benzaldehyde into the CTH system, benzaldehyde demonstrated high yield of benzyl alcohol (**2f**) and acetal in 88% and 7%, respectively. The production of 1-phenylethanol (**4d**) was limited to only 9%, and no discernible transformation was observed for other functional groups (Fig. 5 and Fig. S8 in Supporting information). It is important to point out that the selective hydrogenation generally occurs between two unsaturated groups. Here, a notable breakthrough is the achievement of highly selective reduction for -CHO groups, even in the presence of various functional groups. Significantly, the precise chemoselectivity among various unsaturated groups demonstrated by catalyst **1** in CTH reactions finds significant prospects in selective reduction fields and industrial production.

Subsequently, an assessment was conducted on the range of aldehydes incorporating various functional groups, taking their electronic effects, steric hindrance, and volumetric dimensions into account (Table 2). Widely studied biomass derived furfural (FUL, **1e**) could be converted to furfural alcohol (FOL, **2e**) in high yield (92%). Benzaldehyde (**1f**) successfully yielded benzyl alcohol (**2f**) with a high yield of 94%. In the case of 2-methylbenzaldehyde (**1g**), the corresponding primary alcohol (**2g**) was obtained with a moderate yield. When it came to *ortho*-halogen substituted benzaldehydes (**1h**-**1j**), the yield decreased as the size of the halogen increased. The disparity in yields observed for *ortho*-substituted groups may be attributed to the varying degrees of steric hindrance and their respective interference with the reaction center, and bulky *ortho*-substituents tend to obstruct the reaction site, thereby inhibiting the yield. 3-Methylbenzaldehyde (**1k**) provided a moderate yield of product **2k** (49%), while 3-bromobenzaldehyde (**1l**) exhibited a high yield in the CTH process (**2l**, 93%). The discrepancy can be attributed to the differing electronic effects of the substituents. 4-Methyl and 4-methoxybenzaldehyde gave the corresponding CTH products **2m**-**2n** in moderate yields, while electron deficient group containing benzaldehydes **1o**-**1q** presented the alcohol products **2o**-**2q** in high yields (93%-99%). Compared to electronic or steric hindrance effect, volumetric effect has a more obvious influence. 1-Naphthaldehyde (**1r**) exhibited a lower yield of 64% in the formation of 1-naphthalenemethanol (**2r**) compared to substrates with smaller sizes. 4-Phenylbenzaldehyde (**1s**) produced the alcohol **2s** in 60% yield due to the larger size. When larger-sized substrates, such as **1t** and **1u**, were chosen for transfer hydrogenation reactions, the yields further decreased to 19% and 20% respectively. The significantly bulky substrate **1v** only achieved the target primary alcohol product with a yield of 10% under standard conditions, leaving a substantial amount of starting material unused. Therefore, this catalytic system exhibits excellent selectivity towards the size of aldehyde substrates and can be utilized for the efficient screening of reactants suitable for the reaction.

After condition optimization using acetophenone (**3d**) as the model substrate (Tables S5-S9 and Table 3, entry 1), various ketones were evaluated in CTH reactions with **1** as the catalyst and *i*PrOH as the hydrogen source at 120 °C for 24 h (Table 3). 2-Methylacetophenone (**3e**) gave the corresponding reduction product **4e** in 58% yield, which was possibly due to the bulky steric hindrance around the reactive center and the difficulty of approaching the catalytic sites. When 4-methylacetophenone (**3f**) was introduced to this reaction, product **4f** could be obtained in 76% yield, and an elevated value of 88% could be realized when extended to 36 h. *para*-Halogen group-containing acetophenones **3g**-**3i** underwent the CTH process smoothly, and presented corresponding alcohol products **4g**-**4i** in high yields (94%). *N*–Heterocyclic ketones **3j**-**3k** were also examined, with the result that 2- and 4-acetylpyridine showed excellent activity to give **4j** and **4k** in 92% and 99% yields. Aliphatic cyclic ketones also exhibited efficient activities. Cyclopentanone and cyclohexanone (**3l** and **3m**) both exhibited excellent yields of 99% to give cyclopentanol and cyclohexanol (**4l** and **4m**), respectively. Ascribed to the bulky size, benzophenone (**3n**) and 1-phenyl-1-butanone (**3o**) delivered the alcohol products **4n** and **4o** in reduced yields of 62% and 61%. When larger-sized ketones were introduced, the yields exhibited a more significant decrease. 4,4′-Dimethylbenzophenone (**3p**) could realize the CTH reaction, but produced the product **4p** in 40% yield. The lager-sized 4-benzoylbiphenyl (**3q**) afforded the desired CTH prod-

Table 2
Substrate scope of aldehydes.[a]

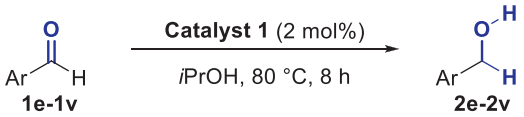

Entry	Substrate	Size	Yield (%)	Entry	Substrate	Size	Yield (%)
1	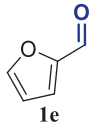 1e	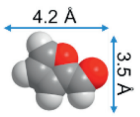 4.2 Å × 3.5 Å	92	10	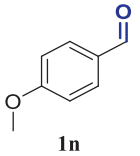 1n	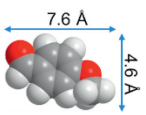 7.6 Å × 4.6 Å	61
2	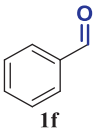 1f	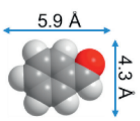 5.9 Å × 4.3 Å	94	11	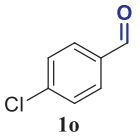 1o	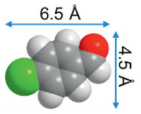 6.5 Å × 4.5 Å	96
3	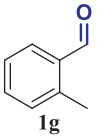 1g	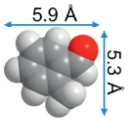 5.9 Å × 5.3 Å	68	12	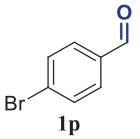 1p	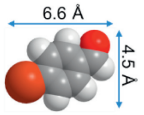 6.6 Å × 4.5 Å	99
4	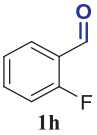 1h	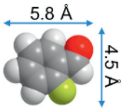 5.8 Å × 4.5 Å	97	13	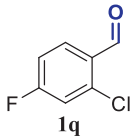 1q	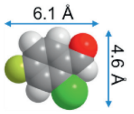 6.1 Å × 4.6 Å	93
5	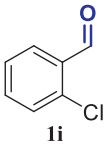 1i	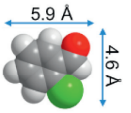 5.9 Å × 4.6 Å	89	14	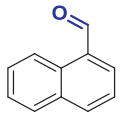 1r	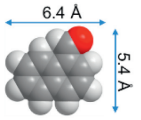 6.4 Å × 5.4 Å	64
6	 1j	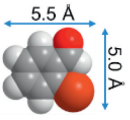 5.5 Å × 5.0 Å	70	15	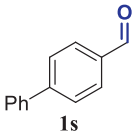 1s	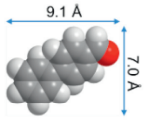 9.1 Å × 7.0 Å	60
7	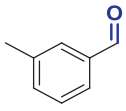 1k	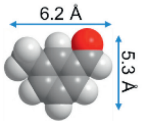 6.2 Å × 5.3 Å	49	16	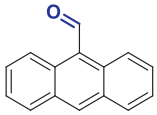 1t	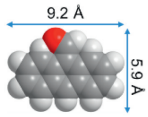 9.2 Å × 5.9 Å	19
8	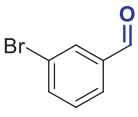 1l	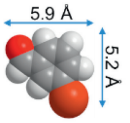 5.9 Å × 5.2 Å	93	17	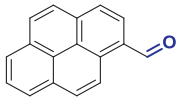 1u	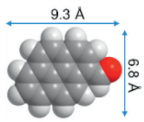 9.3 Å × 6.8 Å	20
9	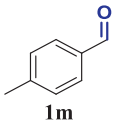 1m	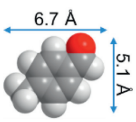 6.7 Å × 5.1 Å	64	18	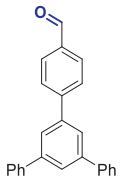 1v	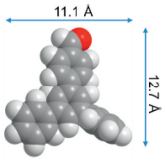 11.1 Å × 12.7 Å	10

[a] Reaction conditions: aldehydes (0.3 mmol), **1** (2 mol%), *i*PrOH (2 mL), 80 °C, 8 h, isolated yields.

Table 3
Substrate scope of ketones.[a,b]

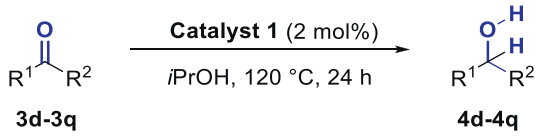

Entry	Substrate	Size	Yield (%)	Entry	Substrate	Size	Yield (%)
1	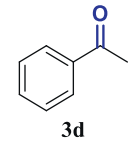 **3d**	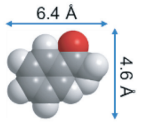	97	8	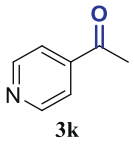 **3k**	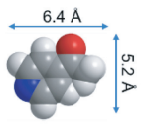	99
2	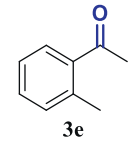 **3e**	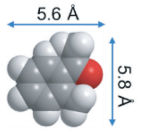	58	9	 **3l**	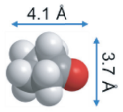	99
3	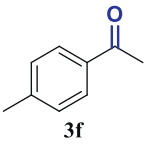 **3f**	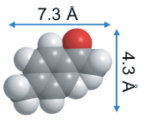	88[b]	10	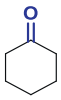 **3m**	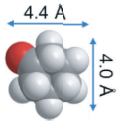	99
4	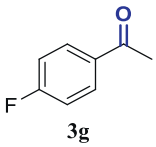 **3g**	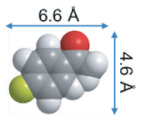	94	11	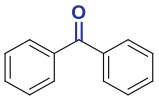 **3n**	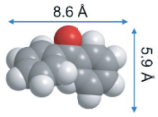	62
5	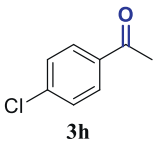 **3h**	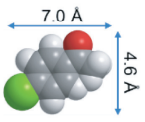	94	12	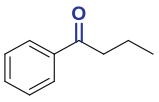 **3o**	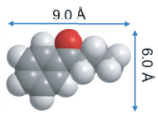	61
6	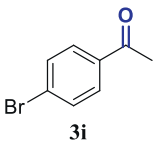 **3i**	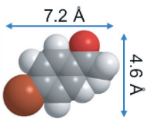	94	13	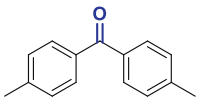 **3p**	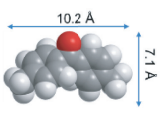	40
7	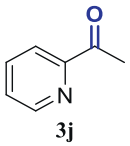 **3j**	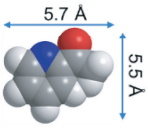	92	14	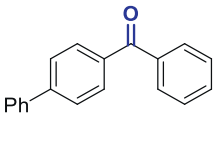 **3q**	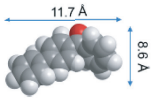	28

[a] Reaction conditions: ketones (0.3 mmol), **1** (2 mol%), *i*PrOH (1 mL), 120 °C, 24 h, isolated yields.
[b] 36 h.

uct **4q** in only 28% yield, indicating obvious size selectivity for the substrates.

As the reaction time increased, obvious gradual consumption of the substrates and generation of the reduction products can be observed by ^{1}H NMR analysis (Fig. 6a and Fig. S9 in Supporting information). Using acetophenone **3d** as an example, the CTH exhibited rapid progress within the first 2 h, followed by a slower rate up to 12 h (Fig. 6b, blue line). Unlike the continuous formation of the product observed in the catalyst-induced system, the reductive product **4d** was not obtained upon removing the catalyst from the system after a 4-h reaction, indicating the essential role and high stability of the catalyst (Fig. 6b, pink line). The yield of CTH product remained remarkably high even after the catalyst employed for at least 6 times, showing high catalytic performance and recyclability of **1** (Fig. 6c and Fig. S10 in Supporting information). ICP-OES analysis indicated the contents of Zr and In of the used catalyst

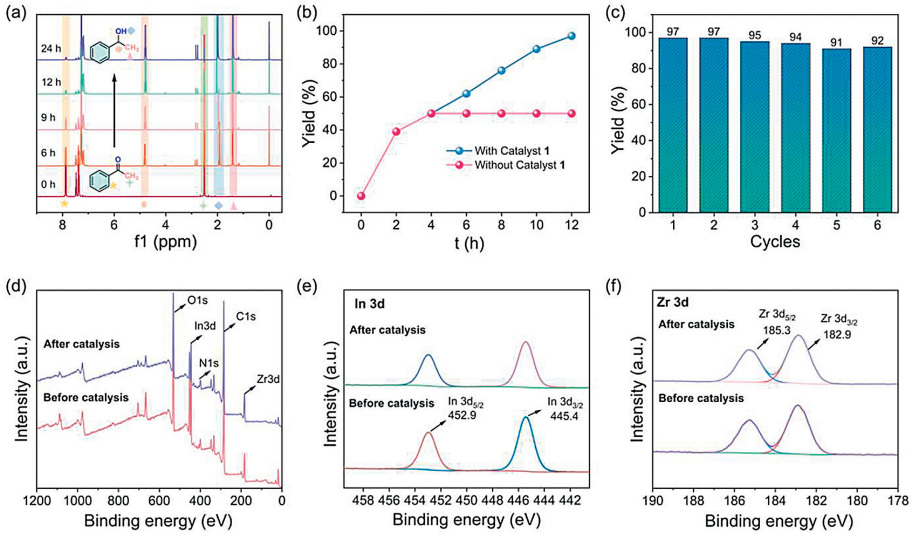

Fig. 6. (a) Monitoring the CTH of acetophenone (**3d**) for different reaction time. (b) Yield-time curve (**3d**) and the leaching test. (c) Catalytic results for CTH of **3d** after catalyst reused successive 6 times. (d-f) Compared XPS spectra of **1** before and after catalysis.

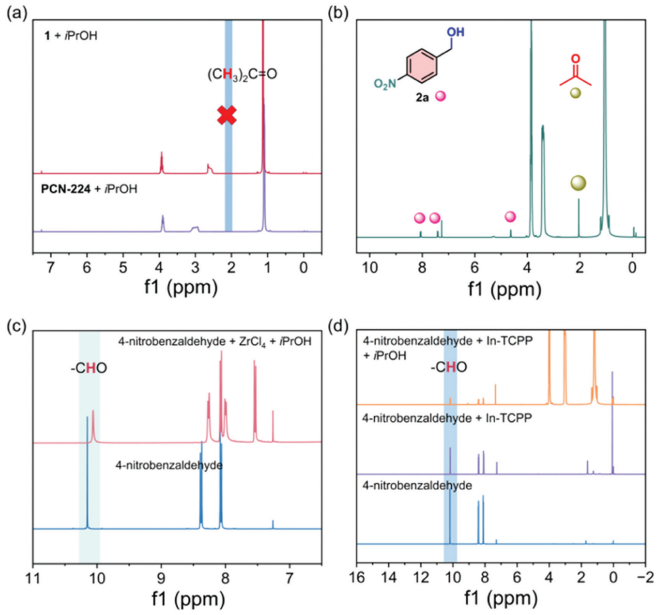

Fig. 7. Control experiments detected by ^{1}H NMR analysis. (a) None acetone generation after mixing of *i*PrOH with **1** or PCN-224. (b) *In-situ* CTH reaction of 4-nitrobenzaldehyde (**1a**) in NMR tube. (c) ^{1}H NMR spectra for interaction of **1a**, $ZrCl_4$ and *i*PrOH. (d) ^{1}H NMR spectra for interaction of **1a**, In-TCPP and *i*PrOH.

were 16.2% and 4.98% respectively, only slightly losing compared with the fresh **1** (15.5% for Zr, 5.78% for In). Additionally, XPS signals and PXRD peaks were almost identical between the fresh and recycled catalyst (Figs. 6d-f and Fig. S11 in Supporting information). The results above demonstrated the outstanding stability, recyclability and catalytic activity of the heterogeneous catalyst **1**.

To gain a deeper understanding of the mechanism underlying activity and selectivity of the CTH process, we carried out control experiments and density functional theory (DFT) calculations (Figs. 7 and 8, Fig. S12 in Supporting information). No detectable acetone signal was generated according to ^{1}H NMR analysis even over a prolonged period when PCN-224 or catalyst **1** was combined with *i*PrOH, but the *in-situ* CTH reaction of **1a** afforded product **2a** and acetone (Figs. 7a and b), which ruled out the possibility of metal hydride serving as an intermediate in this process and determined the transfer hydrogenation mediated by *i*PrOH. The corresponding hydrogen signals shifted significantly when mixing *i*PrOH and $ZrCl_4$ (Fig. S12 in Supporting information). Furthermore, the -CHO hydrogen signal experienced a significant shift when $ZrCl_4$ and **1a** were introduced to *i*PrOH (Fig. 7c). Whereas in both these scenarios, the -CHO hydrogen signal remained original state when either **1a** and In-TCPP or **1a**, In-TCPP and *i*PrOH were combined (Fig. 7d). These observations imply that the Zr_6O_8 cluster engages in interactions with both *i*PrOH and aldehyde group, and serves as the catalysis center, whereas the In-porphyrin component does not participate in such interactions. However, In-TCPP may interact with -NO_2 and other unsaturated groups within the substrates [58], constituting different functions of the porphyrin metal centers and the Zr_6O_8 nodes within catalyst **1**. These results constitute the fundamental reason for the observed chemoselectivity, and the multiple Lewis acid centers also promote the substrates into the channels and accelerate the reaction rate.

DFT calculations were firstly conducted to explore the reaction among Zr_6O_8 node, **1a**, and *i*PrOH, with the corresponding energy profile (ΔG) depicted in Fig. 8a. In the initial step, the -OH group of *i*PrOH underwent deprotonation by the -OH within the Zr_6O_8 node, resulting in the attachment of the deprotonated *i*PrOH to Zr_6O_8 node (+0.41 kcal/mol, **Int-1**). Subsequently, the aldehyde group of **1a** displaced the water molecule of the cluster (+3.92 kcal/mol, **Int-2**). Transfer hydrogenation took place from the tertiary carbon of the deprotonated *i*PrOH to the carbon of -CHO group through transition state **Ts-1**, and a high activation energy of +13.22 kcal/mol with a substantial energy barrier signifies that this step is the rate-determining step. The reaction energy decrease for acetone and benzyl oxygen anion interacting with the Zr_6O_8 node (**Ts-1** → **Int-3**) was estimated to be highly exothermic by −19.94 kcal/mol. Subsequently, the acetone was substituted with a second *i*PrOH, leading to a substantial exothermic process of −5.46 kcal/mol (**Int-4**). The second transfer hydrogenation process occurred from the -OH group of *i*PrOH to benzyl oxygen anion (**Ts-2**) with a low energy barrier of +0.68 kcal/mol and affording **Int-5**. However, the energy gap in this step was notably lower than **Ts-1**. Following this, upon the replacement by H_2O, product **2a** was afforded and **Int-1′** was regenerated to complete the catalytic cycle.

The DFT calculations were further investigated among Zr_6O_8 node, **3a**, and *i*PrOH under the same conditions as **1a** system

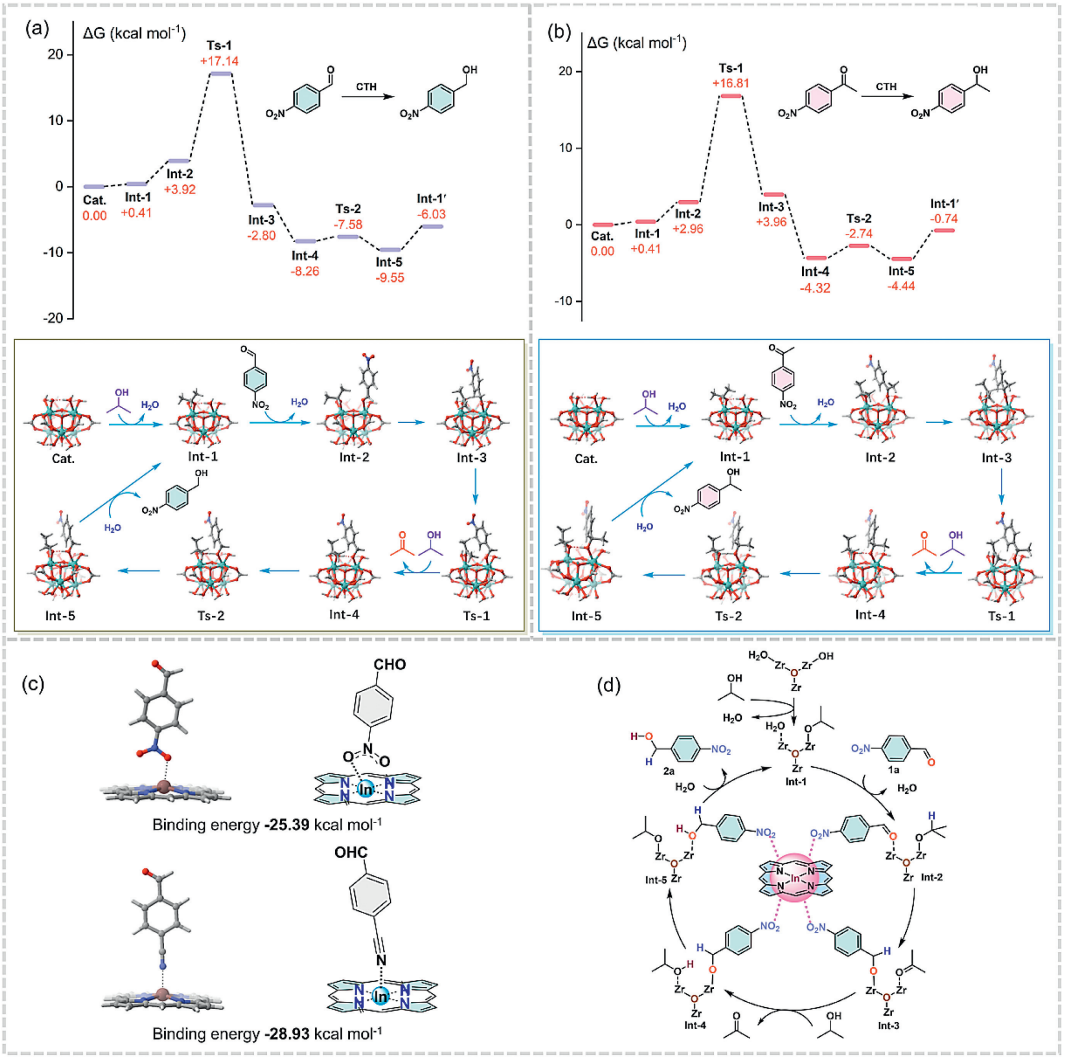

Fig. 8. (a) Reaction energies for CTH of **1a** calculated by DFT. (b) Reaction energies for CTH of **3a** calculated by DFT. (c) Binding energies of In-TCPP with -NO_2 and -CN for corresponding aldehydes. (d) Proposed CTH mechanism towards the example of **1a**.

(Fig. 8b). The activated energies for **Ts-1** and **Ts-2** were determined to be 13.85 and 1.58 kcal/mol, respectively. Notably, the energy value for **Ts-2** of -$COCH_3$ was significantly higher compared to that of -CHO (+0.68 kcal/mol), whereas the energy value of **Ts-1** was relatively similar. Moreover, the corresponding reaction energies required for the first hydrogen transfer process (**Int-2** → **Int-3**) with **3a** as substrate was much higher than that of **1a**. The above results suggest that the CTH conversion of -$COCH_3$ is more challenging than that of -CHO, providing a reasonable insight into the high selectivity between -CHO and -$COCH_3$ in CTH reaction. To elucidate other chemoselectivity, we conducted interaction calculations involving **1a** and **1b** with In-TCPP. The binding energies for -NO_2 and -CN with the porphyrin central metal were determined to be −25.39 and −28.93 kcal/mol, respectively (Fig. 8c). The above-mentioned results indicate that -NO_2 and -CN exhibit strong interactions with the In-porphyrin moiety, whereas -C=O displays a greater affinity for the Zr_6O_8-based CTH catalytic center. Thus, the chemoselectivity arises from the distinct Lewis acid center-substrate group interactions. Furthermore, both Zr_6O_8 nodes and In-porphyrin moieties facilitate preferential enrichment of reactants, promoting the catalytic process for the CTH reaction. Therefore, the proposed mechanism (Fig. 8d), highlights that Zr_6O_8 clusters serve as the catalytic sites and the In-porphyrin acts as the Lewis acid binding site, playing an important role in enhancing activity and chemoselectivity during the CTH process.

In summary, a new In-captured Zr-porphyrin framework (**1**) assembled by Zr_6O_8 clusters and In-porphyrin moieties was successfully constructed. **1** displayed highly multi-selective CTH of aldehydes and ketones containing both chemo- and size selectivity. Based on catalyst **1**, C=O bonds in aldehydes and ketones could be selectively reduced to CH-OH in the presence of other unsaturated groups including -NO_2, -CN, and C=C bonds. Furthermore, through tuning the conditions under the activation of catalyst **1**, high selectivity of 97% towards -CHO was achieved in the concurrent existence of -CHO and -$COCH_3$ groups, whether in intra- or intermolecular settings. Importantly, **1** also exhibited prominent selectivity towards -CHO in the CTH among five types of unsaturated groups mentioned above. Additionally, an obvious size selectivity was achieved, primarily attributed to the well-defined pore size of the catalyst. Control experiments and DFT calculations provided clear evidence that chemoselectivity was mainly controlled by synergistic effect of the Zr and In centers within **1**, and the selectivity towards -CHO in presence of -$COCH_3$ was attributed to the easier realization of transfer hydrogenation processes for -CHO compared to -$COCH_3$. This research represents the first example for realizing multi-selective CTH reactions, combining both chemoselectiv-

ity among many kinds of unsaturated groups and size selectivity for various substrates.

Declaration of competing interest

The authors declare that they have no known competing financial interests or personal relationships that could have appeared to influence the work reported in this paper.

CRediT authorship contribution statement

Hua Liu: Writing – original draft, Investigation, Formal analysis, Data curation. **Jian Zhao:** Software, Investigation. **Qi Li:** Formal analysis, Data curation. **Xiang-Yu Zhang:** Writing – review & editing, Supervision, Funding acquisition, Conceptualization. **Zhi-Wei Zheng:** Software, Formal analysis. **Kun Huang:** Supervision, Funding acquisition. **Da-Bin Qin:** Supervision, Funding acquisition, Conceptualization. **Bin Zhao:** Writing – review & editing, Supervision, Funding acquisition, Conceptualization.

Acknowledgments

This study was financially supported by National Nature Science Foundation of China (Nos. 92161202 and 22121005), China Postdoctoral Science Foundation (Nos. 2023M741814 and 2023M741815), Postdoctoral Fellowship Program of CPSF (No. GZC20231170), Natural Science Foundation of Science & Technology Department of Sichuan Province (No. 2023NSFSC110) and Research and Innovation Team of China West Normal University (No. KCXTD2023-1).

Supplementary materials

Supplementary material associated with this article can be found, in the online version, at doi:10.1016/j.cclet.2024.110593.

References

[1] W. Zuo, A.J. Lough, Y.F. Li, et al., Science 342 (2013) 1080–1083.
[2] M. Zhao, K. Yuan, Y. Wang, et al., Nature 539 (2016) 76–80.
[3] L. Zhang, M. Zhou, A. Wang, et al., Chem. Rev. 120 (2020) 683–733.
[4] Y. Wang, Z. Huang, X. Leng, et al., J. Am. Chem. Soc. 140 (2018) 4417–4429.
[5] L. Wang, J. Lin, Q. Sun, et al., ACS Catal. 11 (2021) 8033–8041.
[6] F. Wang, T. Yang, T. Wu, et al., J. Am. Chem. Soc. 143 (2021) 2477–2483.
[7] X. Li, W. Hao, N. Yi, et al., CCS Chem. 5 (2023) 2277–2289.
[8] D. Wang, D. Astruc, Chem. Rev. 115 (2015) 6621–6686.
[9] Y.Y. Li, S.L. Yu, W.Y. Shen, et al., Acc. Chem. Res. 48 (2015) 2587–2598.
[10] Z. An, J. Li, Green Chem. 24 (2022) 1780–1808.
[11] A.H. Valekar, M. Lee, J.W. Yoon, et al., ACS Catal. 10 (2020) 3720–3732.
[12] J. Wei, L. Zhao, C. He, et al., J. Am. Chem. Soc. 141 (2019) 12707–12716.
[13] R.A. Farrar-Tobar, A. Dell'Acqua, S. Tin, et al., Green Chem. 22 (2020) 3323–3357.
[14] S.M. King, X. Ma, S.B. Herzon, J. Am. Chem. Soc. 136 (2014) 6884–6887.
[15] C.K. Hill, J.F. Hartwig, Nat. Chem. 9 (2017) 1213–1221.
[16] Y. Ren, Y. Yang, M. Wei, ACS Catal. 13 (2023) 8902–8924.
[17] W. Gong, X. Chen, W. Zhang, et al., J. Am. Chem. Soc. 144 (2022) 3117–3126.
[18] X.R. Tian, Z.Y. Jiang, S.L. Hou, et al., Angew. Chem. Int. Ed. 62 (2023) e202301764.
[19] G.D. Wang, Y.Z. Li, W.J. Shi, et al., Angew. Chem. Int. Ed. 62 (2023) e202311654.
[20] L. Sun, X. He, Y. Yuan, et al., Chem. Eng. J. 397 (2020) 125468.
[21] K. Sun, Y. Qian, H.L. Jiang, Angew. Chem. Int. Ed. 62 (2023) e202217565.
[22] C.P. Wang, Y.X. Lin, L. Cui, et al., Small 19 (2023) 2207342.
[23] E.X. Chen, M. Qiu, Y.F. Zhang, et al., Angew. Chem. Int. Ed. 61 (2022) e202111622.
[24] X. Chen, C. Peng, W. Dan, et al., Nat. Commun. 13 (2022) 4592.
[25] Q. Wu, A. Li, R. He, et al., Chin. Chem. Lett. 35 (2024) 108639.
[26] X. Kou, Y. Lin, Y. Shen, et al., CCS Chem. 6 (2024) 1821–1835.
[27] R.J. Wei, H.G. Zhou, Z.Y. Zhang, et al., CCS Chem. 3 (2021) 2045–2053.
[28] M. Zhao, S. Huang, Q. Fu, et al., Angew. Chem. Int. Ed. 59 (2020) 20031–20036.
[29] K. Sheng, L.M. Fan, X.F. Tian, et al., Sci. Chin. Chem. 63 (2020) 182–186.
[30] L. Yang, P. Cai, L. Zhang, et al., J. Am. Chem. Soc. 143 (2021) 12129–12137.
[31] X.C. Lin, Y.M. Wang, X. Chen, et al., Angew. Chem. Int. Ed. 62 (2023) e202306497.
[32] F. Guo, R.X. Li, S. Yang, et al., Angew. Chem. Int. Ed. 62 (2023) e202216232.
[33] X.S. Jiang, F.Y. Ren, Y. Shi, et al., CCS Chem. 6 (2024) 2333–2345.
[34] X.S. Li, J. Zhao, S.L. Hou, et al., CCS Chem. 6 (2024) 2982–2995.
[35] X.S. Li, J. Zhao, L. Luo, et al., Chin. Chem. Lett. 35 (2024) 109407.
[36] Y.S. Wei, M. Zhang, R. Zou, et al., Chem. Rev. 120 (2020) 12089–12174.
[37] T. He, X.J. Kong, J.R. Li, Acc. Chem. Res. 54 (2021) 3083–3094.
[38] Y. Song, X. Feng, J.S. Chen, et al., J. Am. Chem. Soc. 142 (2020) 4872–4882.
[39] Q.J. Wu, J. Liang, Y.B. Huang, et al., Acc. Chem. Res. 55 (2022) 2978–2997.
[40] Z. Ji, H. Wang, S. Canossa, et al., Adv. Funct. Mater. 30 (2020) 2000238.
[41] C.X. Chen, Z.W. Wei, T. Pham, et al., Angew. Chem. Int. Ed. 60 (2021) 9680–9685.
[42] G. Ji, L. Zhao, J. Wei, et al., Angew. Chem. Int. Ed. 61 (2022) e202114490.
[43] N. Li, G.Q. Lai, L.H. Chung, et al., CCS Chem. 6 (2023) 1211–1221.
[44] S. Fu, S. Yao, S. Guo, et al., J. Am. Chem. Soc. 143 (2021) 20792–20801.
[45] P. Vasanthakumar, D.S. Raja, D. Sindhuja, et al., Mol. Catal. 516 (2021) 112004.
[46] D. Feng, W.C. Chung, Z. Wei, et al., J. Am. Chem. Soc. 135 (2013) 17105–17110.
[47] G. Zhai, Y. Liu, L. Lei, et al., ACS Catal. 11 (2021) 1988–1994.
[48] P. Jin, L. Wang, X. Ma, et al., Appl. Catal. B: Environ. 284 (2021) 119762.
[49] M.W. Geis, T.H. Fedynyshyn, M.E. Plaut, et al., Diam. Relat. Mater. 84 (2018) 86–94.
[50] H. Liu, H.J. Li, Z.W. Zheng, et al., Cryst. Growth Des. 23 (2023) 7316–7324.
[51] H. Liu, Z.W. Zheng, X.Y. Zhang, et al., Inorg. Chem. 63 (2024) 11554–11565.
[52] Q. Wang, Z. Wei, J. Li, et al., ACS Appl. Mater. Interfaces 14 (2022) 27775–27790.
[53] F.A. Westerhaus, R.V. Jagadeesh, G. Wienhöfer, et al., Nat. Chem. 5 (2013) 537–543.
[54] J. Zhang, L. Wang, Y. Shao, et al., Angew. Chem. Int. Ed. 56 (2017) 9747–9751.
[55] R.B. Nasir Baig, R.S. Varma, ACS Sustain. Chem. Eng. 1 (2013) 805–809.
[56] W. Walczak, M. Zakrzewski, G. Cichowicz, et al., Org. Biomol. Chem. 18 (2020) 694–699.
[57] Z.W. Xi, L. Yang, D.Y. Wang, et al., J. Org. Chem. 86 (2021) 2474–2488.
[58] Y. Li, Y.N. Li, J.W. Zheng, et al., Chem. Eur. J. 27 (2021) 1080–1087.